AAPS PharmSciTech (2019) 20: 289
DOI: 10.1208/s12249-019-1502-0

Check for updates

Research Article

Exploring the Potential of Mesoporous Silica as a Carrier for Puerarin: Characterization, Physical Stability, and *In Vivo* Pharmacokinetics

Zhi Wang,[1] Bei-Ni Ye,[1,2] Yong-Tai Zhang,[1] Jian-Xu Xie,[1] Wan-Si Li,[1] Hong-Tao Zhang,[3] Ying Liu,[1] and Nian-Ping Feng[1,4]

Received 13 April 2019; accepted 5 August 2019; published online 14 August 2019

Abstract. The aim of this study was to evaluate the use of a novel porous silica carrier, AEROPERL® 300 Pharma (AP), to improve the *in vitro* release and oral bioavailability of puerarin (PUE) in solid dispersions (SDs). PUE-AP SD formulations with different ratios of drug to silica (RDS) were prepared by the solvent method. The scanning electron microscopy (SEM) results indicated that the dispersion of PUE improved as the concentration of AP was increased. The differential scanning calorimetry (DSC) and X-ray diffraction (XRD) results revealed that PUE mostly existed in an amorphous state in the SDs. The rate of drug dissolution from the SDs was significantly higher than that from the PUE powder ($p < 0.05$). The *in vitro* drug release percentage from the PUE-AP SDs increased as the RDS was reduced. The oral bioavailability of PUE from the SDs improved when using AP, as indicated by $AUC_{(0-\infty)}$, which was 2.05 and 2.01 times greater than that of the PUE (API) and PVP K30 SDs, respectively ($p < 0.05$). The drug content, *in vitro* release profiles, and the amorphous state of PUE in the PUE-AP SDs showed no significant changes after being stored at room temperature for 6 months or under accelerated conditions (40 ± 2°C, 75 ± 5% relative humidity) for 3 months. AP has a high pore volume, large specific surface area, excellent flowability, and hydrophilic properties, making it capable of improving the dissolution and bioavailability of poorly water-soluble drugs.

KEY WORDS: AEROPERL® 300 Pharma; puerarin; solid dispersion; physical stability; bioavailability.

INTRODUCTION

Silica is an important excipient that is inert and generally regarded as safe (GRAS) [1]. It is commonly used in pharmaceutics as an adsorbent and a glidant, thickener, and suspending agent, in addition to other applications [2]. To expand its scope of use, silica has been variably modified to impart novel physical properties [3], including the application of porous silica (PS) to enhance the dissolution of poorly water-soluble drugs. PS (Sylysia 350) has been previously used to improve the dissolution rate of carvedilol [4] and enhance the dissolution and oral bioavailability of the cytokine K-832 (2-benzyl-5-(4-chlorophenyl)-6-[4-(methylthio)phenyl] -2H-pyridazin-3-one) by adsorbing it onto PS (Sylysia 350) using supercritical carbon dioxide [5]. Silica nanoparticles and ordered mesoporous silica containing pores with diameters ranging between 2 and 50 nm are also being explored as drug carriers to enhance the dissolution and absorption characteristics of drugs with poor water solubility [6–8].

AEROPERL® 300 Pharma (AP) is a highly purified (99.8% w/w), amorphous, anhydrous, and colloidal silicon dioxide with a high pore volume and large specific surface area. It consists of spherical granules with particles of medium diameter, ranging between 30 and 40 μm. Its spherical structure allows for excellent flowability, resulting in improved mixing and flow properties of the powder during pelleting and tableting compared with those of conventional PS [9]. Recent reports have demonstrated that AP exhibits an excellent potential to act as a solubility modulator by forming a solid dispersion (SD) [10]. When using AP as drug carriers, the drug release rate of bicalutamide (BCL) was enhanced approximately 15 times compared to that of neat BCL. This improvement may be attributed to the high surface area, improved wettability of AP, and decreased crystallinity of active pharmaceutical ingredients (APIs) [2]. The pore volume of AP is as high as 1.6 mL/g, and it can be loaded with drug molecules. Additionally, it has a large specific

[1] Department of Pharmaceutical Sciences, School of Pharmacy, Shanghai University of Traditional Chinese Medicine, 1200 Cailun Road, Zhangjiang Hi-Tech Park, Pudong New District, Shanghai, 201203, China.
[2] Preparation Department, Hangzhou Qingyue Pharmaceutical Technology Co., Ltd., Hangzhou, Zhejiang, China.
[3] Resource Efficiency, Evonik Specialty Chemicals (Shanghai) Co., Ltd., Shanghai, China.
[4] To whom correspondence should be addressed. (e–mail: npfeng@hotmail.com; npfeng@shutcm.edu.cn)

surface area, up to 300 m^2/g, which is conducive to the formation of contacts with water and can thus improve the dissolution rate [11]. In addition, the Si–OH groups on its surface can form hydrogen bonds with drug molecules [12]. The drug is therefore expected to be molecularly dispersed on the surface of AP, which in turn would enhance its dissolution.

Puerarin (7,4′-dihydroxyisoflavone-8-β-D-glucopyranoside, PUE, Fig. 1a) is an active isoflavone extracted from the traditional Chinese herb *Pueraria lobata* (Willd.) Ohwi. PUE has been shown to be effective for the treatment of cardiovascular diseases, liver injury, platelet aggregation disorders, and hyperglycemic disorders, among others [13–15]. However, the water solubility of PUE is poor, at 1.1×10^{-2} mol/L [16], which limits its release from conventional oral preparations such as tablets and granules, resulting in low oral bioavailability.

In this study, an AP-based SD was employed as a vehicle for administering PUE. Various SD formulations with different ratios of drug to silica (RDS) were prepared and subsequently characterized using scanning electron microscopy (SEM), differential scanning calorimetry (DSC), and powder X-ray diffraction (PXRD). The physical stability of the SD formulations was also determined. The dissolution and pharmacokinetic properties in rats of the SDs were also compared with those of SDs prepared using precipitated silica (silica EY-CD1) and PVP K30 as carriers.

MATERIALS AND METHODS

Materials

PUE (certified reference material) was supplied by the National Institute for the Control of Pharmaceutical and Biological Products (Beijing, China). PUE (purity > 98%) was obtained from the Dalian Meilun Biology Technology Co. Ltd. (Dalian, China). AP was a kind gift from Evonik Industries AG (Essen, Germany). PVP K30 was purchased from Sinopharm Chemical Reagent Co. Ltd. (Shanghai, China). Silica EY-CD1 was procured from Anhui Shanhe Pharmaceutical Excipients Co. Ltd., (Huainan, China). The methanol used for high-performance liquid chromatography (HPLC) analysis was obtained from Merck (Darmstadt, Germany). All the other chemicals used in this study were of analytical grade and were used without further purification.

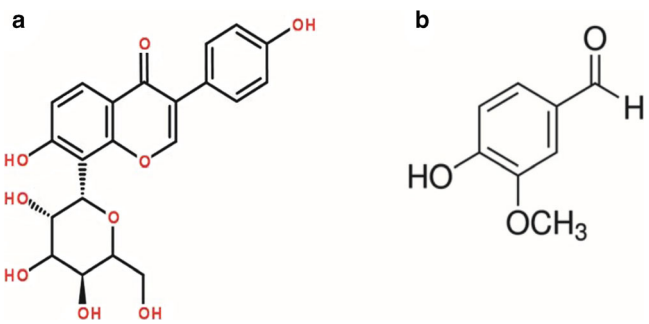

Fig. 1. Chemical structure of puerarin (**a**) and vanillin (**b**)

Animals

Male Sprague–Dawley rats, weighing 180–220 g, were obtained from the Laboratory Animal Center of the Shanghai University of Traditional Chinese Medicine. All the animal experiments were carried out in accordance with the guidelines of the National Act on the Use of Experimental Animals and were approved by the local ethics committee (SCXK:2013-0016).

High-Performance Liquid Chromatography Assay

The concentration of PUE in the samples used for the *in vitro* and *in vivo* studies was determined by HPLC (Agilent 1260 Infinity, Agilent Technologies, Inc., Santa Clara, CA, USA) using a reverse phase Athena-C18 column (250 × 4.6 mm, 5 μm; CNW Technologies GmbH, Düsseldorf, Germany). The mobile phase consisted of methanol and 0.5% (v/v) aqueous solution of acetic acid at a ratio of 27:73 (v/v), and the flow rate was set at 1.0 mL/min. The wavelength of the ultraviolet detector was set at 250 nm, and the elution temperature was 30°C.

Samples from *in vitro* studies were filtered through 0.45 μm membrane filters before assay, and the retention time of PUE was found to be approximately 13.7 min (Fig. 2). The drug concentration (C) *versus* the corresponding chromatographic peak area (A) showed good linearity within the range of 0.0350–0.6304 mg/mL, and the linear equation was $A = 44172C + 40.811$ ($r = 1.0000$). The relative standard deviation (RSD) of the intraday and interday precision results were less than 3%, and the recovery was between 96.01 and 100.84%.

Vanillin (Fig. 1b) was used as an internal standard (IS) for detection of the plasma samples. Plasma endogenous substances in the samples to be tested did not interfere with the detection (in Fig. 3). The calibration curve of plasma PUE concentration in the range of 0.1213–1.8200 μg/mL was fitted as $A = 6.0135C - 0.1663$ ($r > 0.9991$). The intraday and interday precision was less than 4 and 8%, respectively. The RSD of PUE concentration in the plasma samples measured at room temperature for 12 h and after freeze–thawing for 3 days were less than 8 and 12%, respectively. The recovery of PUE from plasma samples ranged between 90.20 and 106.49%. The limits of detection and quantification were 4.3 and 147.5 ng/mL, respectively. The method was thus confirmed to be suitable for assay plasma samples.

Preparation of PUE-AP SDs and the Compared Formulations

Five PUE-AP SD formulations (Table I) with different RDS were prepared using the solvent method [17, 18]. PUE was weighed accurately and dissolved in methanol to obtain a clear solution, after which AP was suspended in dichloromethane (1:20 w/v). The PUE–methanol solution was then added to the AP suspension, and the mixture was sealed and magnetically stirred at 300 rpm (Vortex Genius 3, IKA Works GmbH & Co., Staufen, Germany) for 1 h at room temperature. The suspension was subsequently transferred to a rotary evaporator (R206 SENCO [GG17], SENCO Technology Co., Ltd., Shanghai, China) and vacuum dried at 45–50°C. The obtained powder was stored in a desiccator for subsequent experiments.

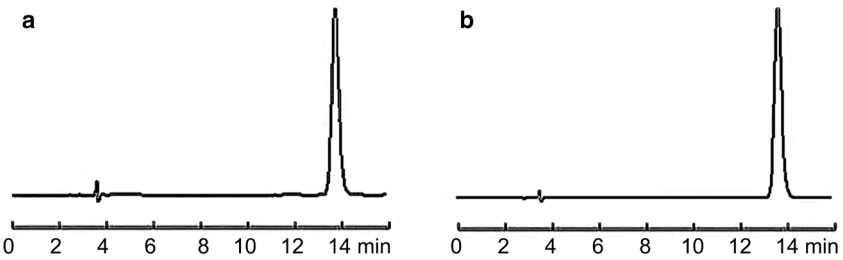

Fig. 2. The chromatogram of PUE reference (**a**) and crude drug (**b**)

Silica EY-CD1 and PVP K30 were individually used to prepare the two types of SDs for comparison. The same preparation method used for PUE-AP SDs was used to prepare PUE-loaded EY-CD1 SDs (PUE-YE-CD1 SDs) with an RDS of 1:3. The PUE-PVP SDs with an RDS of 1:3 were also prepared by the solvent method. Briefly, PUE was weighed accurately and dissolved in ethanol (1:3 w/v) to obtain a clear solution, PVP K30 was then added, and the mixture was magnetically stirred at room temperature for 1 h. The solution was then transferred to a rotary evaporator to remove the majority of the solvent, refrigerated at 4°C, and kept at room temperature to obtain an opaque paste. The paste was subsequently vacuum dried at 40°C and ground into a fine powder.

The physical mixture (PM) was prepared by mixing the necessary amount of PUE and the excipients in a mortar until a homogeneous mixture was obtained.

The prepared formulations were all ground into a fine powder and sifted through a 60-mesh sieve.

Characteristics of SDs

SEM

Environmental scanning electron microscopy (Phillips XL30 ESEM, FEI Co., Hillsboro, OR., USA) was conducted to assess the morphology of the powder samples. All samples were sputter coated with gold before examination. The operating voltage was 20 kV. The samples were observed at ×1000 magnification.

DSC

The PUE-loaded formulations were subjected to thermal investigation using a differential scanning calorimeter (NETZSCH DSC204 F1, NETZSCH-Gerätebau GmbH, Selb, Germany). The sample (2–6 mg) was placed in an aluminum pan with a pierced lid and heated from 30 to 300 K at a rate of 10 K/min. Nitrogen was used as the purge gas, and the flow rate was 60 mL/min.

XRD

The XRD studies were carried out using an X-ray diffractometer (Bruker D8 Advance, Bruker AXS GmbH, Karlsruhe, Germany) with Cu Kα radiation at 40 mA and 40 kV. The diffraction angles were scanned from 3° to 45° (2θ) with a step size of 0.02°, over a counting time of 23.7 s.

In Vitro Release

The *in vitro* release of PUE powder and PUE-AP SDs was assessed in a dissolution apparatus (RC806 Dissolution tester, Tianda Tianfa Technology Co., Ltd., Tianjin, China) according to the operation instructions for the USP Dissolution Test Apparatus 2 (Paddle Apparatus). Samples containing 100 mg of PUE were added to 900 mL of distilled water to meet the sink condition of 37 ± 0.5°C and subsequently stirred at 50 rpm. The dissolution medium (5 mL) was removed and immediately replaced with an equal volume of fresh medium at 5, 10, 15, 30, and 60 min time intervals. The samples were assayed by HPLC.

Drug Content

An appropriate amount of PUE-AP SDs was weighed accurately and extracted with 50 mL of ethanol/water (30:70, v/v) in an ultrasonic bath for 15 min at room temperature. The solution was filtered through a 0.45-μm microporous membrane prior to injection into the HPLC apparatus for analysis.

Stability

The stability of PUE-AP SD formulations was evaluated under accelerated conditions (40 ± 2°C, 75 ± 5% relative humidity (RH)) for 3 months. At each of the predetermined time points, 0, 1, 2, and 3 months, each sample was removed and evaluated for appearance, drug content, and drug dissolution rate. A long-term study was also performed, wherein the PUE-AP SDs were stored at room temperature

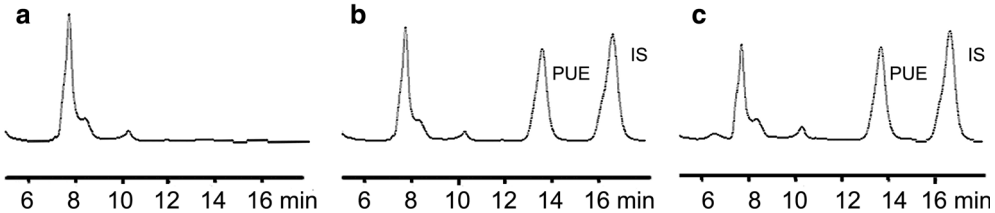

Fig. 3. The chromatogram of blank plasma (**a**), plasma with reference substance (**b**), and plasma sample obtained from rats (**c**)

Table I. PUE-AP SD Formulations

Formulations	PUE (g)	AP (g)
SD 1:1	1.0	1.0
SD 1:2	1.0	2.0
SD 1:3	1.0	3.0
SD 1:5	1.0	5.0
SD 1:10	1.0	10.0

PUE, puerarin; *AP*, AEROPERL® 300 Pharma; *SD*, solid dispersion

for 6 months, and the appearance, drug content, and drug dissolution rate of the samples were determined at 0 and 6 months. The similarity factor (f_2) was calculated for assessing and comparing the dissolution profiles. The results were considered significant when the value of f_2 was less than 50.

The SDs with RDS of 1:3 and 1:10 were simultaneously characterized in DSC and XRD studies after they were stored for 6 months at room temperature.

Determination of Flow Property and Hygroscopic Rate

The flowability of the SD powders was determined using Carr's compressibility index (CI), expressed as a percentage, and the angle of repose. A weighed quantity of the prepared mixtures was poured into a 100-mL cylinder, after which the poured bulk volume (V_b) and tapped volume (V_t) were determined after a sufficient number of taps. The poured bulk density (P_b) and tapped density (P_t) were calculated from the obtained values of V_b and V_t. The CI of each of the powder was calculated using Eq. (1). The angle of repose was measured using a BT-1000 Powder Integrative Characteristics Tester (BT, Dandong, China). The hygroscopicity rate of the SDs was determined using the following steps: a weighing bottle was placed in a desiccator which contained a supersaturated sodium chloride solution on the bottom and was kept at 25 ± 2°C. After 24 h, this bottle was weighed (W_1), and a 1-mm-thick layer of the tested formulations was added to the bottle, which was then weighed (W_2). The bottle containing the SDs was weighed after being stored for 72 h under the constant temperature and humidity conditions mentioned above (W_3). The hygroscopicity rate of the SD powders was calculated using Eq. (2).

$$\mathrm{CI}\% = [(P_t - P_b)/P_t] \times 100 \quad (1)$$

$$\text{Hygroscopic rate}\,(\%) = [(W_3 - W_2)/(W_2 - W_1)] \times 100 \quad (2)$$

Determination of Residual Organic Solvents

Organic reagents, including methanol, dichloromethane, and ethanol, were used in the preparation of the solid dispersion, so the residual organic solvents in the SDs were detected by headspace gas chromatography with a flame ionization detector (HS GC-FID). The chromatographic system used was an HS GC-FID Agilent 7890B, equipped with a flame ionization detector and coupled to an Agilent 7679A headspace injector capable of injecting 1 mL of sample. An Agilent DB-624 capillary column (30 m × 0.32 mm × 1.8 μm) was used. The oven temperature was held at 80°C for 8 min, increased at 20°C/min to 200°C, and finally held for 5 min at this temperature (total run time of 19 min). The injector temperature was maintained at 200°C with a split ratio of 10:1. The detectors were held at 250°C. The following gas flow rates were used: 30.0 mL/min for hydrogen, 400.0 mL/min for air, and 25.0 mL/min for nitrogen. The carrier gas was helium, and its rate was kept constant (2.7 mL/min). An appropriate amount of SDs (about 1 g) was weighed accurately and dispersed in 9 mL of *N,N*-dimethylformamide. The obtained sample was injected into the headspace, separated by gas chromatography, detected using the FID, and quantified using the external standards method.

In Vivo Pharmacokinetic Study

The rats were divided into four groups, with six animals in each group. The animals were fasted overnight and allowed *ad libitum* access to water prior to treatment. The API (PUE, sifted through a 60-mesh sieve) and SDs formulated with an RDS of 1:3 were each mixed with the same volume of water and immediately orally administered to the rats at a dose of 100 mg/kg. Blood samples were collected at predetermined time points after dosing.

The plasma was obtained by centrifugation at 5000 rpm for 10 min. Perchloric acid (160 μL, 6% [v/v]) was added to 200 μL of the plasma and vortex mixed (RCT basic, IKA Works GmbH & Co., Staufen, Germany) for 5 min to precipitate the protein. The sample was then centrifuged (MiniSpin, Eppendorf AG, Hamburg, Germany) at 13,000 rpm for 10 min, and the supernatant was filtered through 0.45 μm membrane filters for HPLC analysis.

Statistical Analysis

The results are presented as the mean ± standard deviation. The comparisons were performed using ANOVA with SPSS software (version 19.0; IBM, Armonk, NY, USA). A p value < 0.05 was considered to indicate statistical significance. The plasma concentration–time data were analyzed with DAS software, version 2.1.1 (Mathematical Pharmacology Professional Committee of China, Shanghai, PCR). The pharmacokinetic parameters were analyzed using noncompartmental analyses.

RESULTS

Characteristics of the Prepared PUE-AP SDs

Figure 4 shows SEM images of the various formulations. The PUE powders (a) have large crystalline particles with cubic shape blocks. AP (b) has a smooth surface with a porous structure and spherical shape. In the SEM image of PM (c), several crystalline drug particles scattered around AP can be seen, while more amorphous PUE was observed on

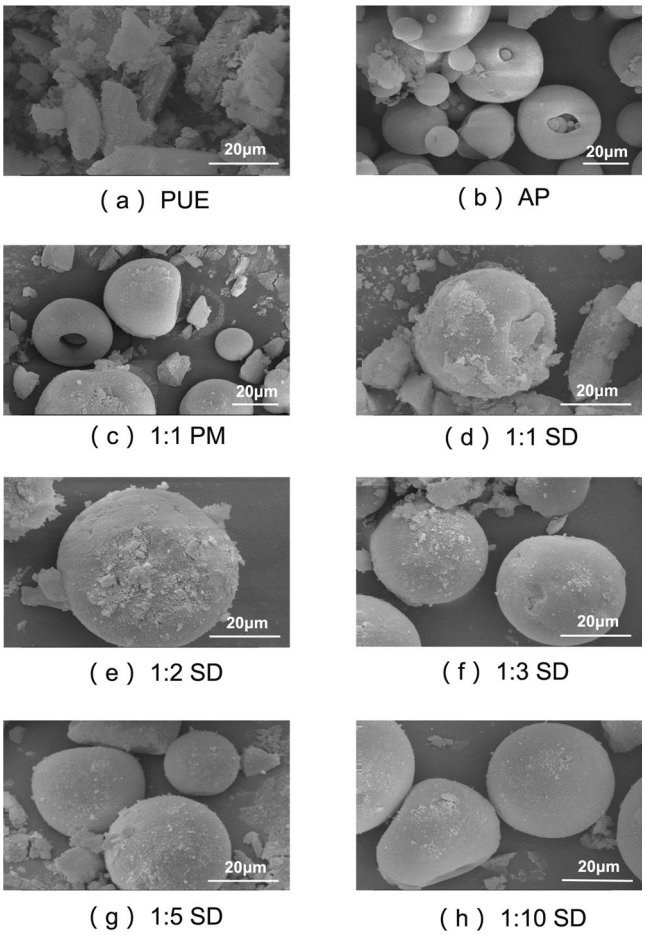

Fig. 4. Scanning electron microscopy photomicrographs of **a** PUE; **b** AEROPERL® 300 Pharma (AP); **c** PUE-AP PM with the ratio of drug to silica (RDS) as 1:1; **d** PUE-AP SD, RDS 1:1; **e** PUE-AP SD, RDS 1:2; **f** PUE-AP SD, RDS 1:3; **g** PUE-AP SD, RDS 1:5; and **h** PUE-AP SD, RDS 1:10. Magnification ×1000

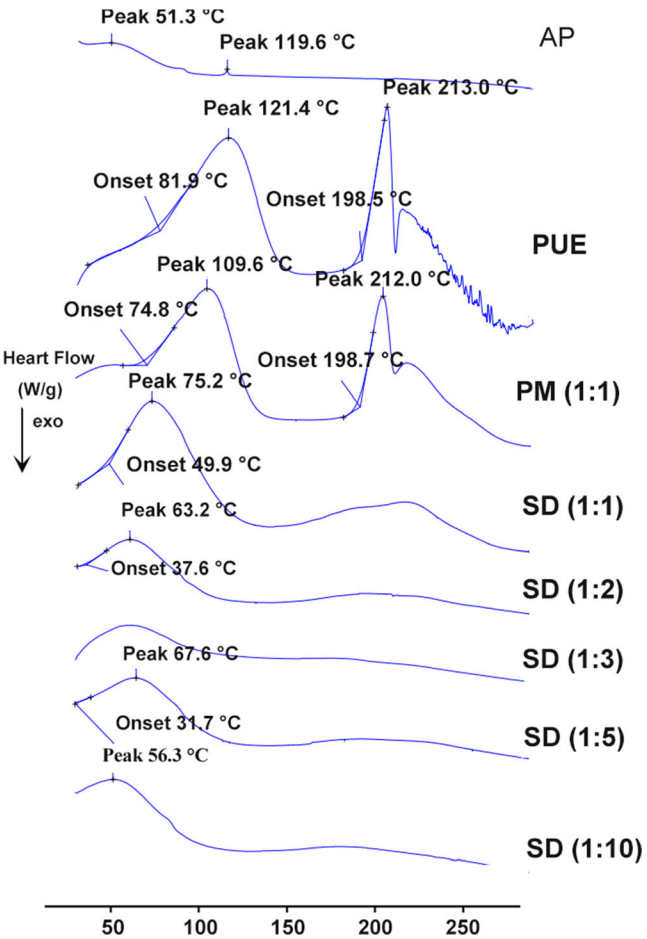

Fig. 5. Differential scanning calorimetry (DSC) curves of PUE, AP, PUE-AP PM, and PUE-AP SDs

the surface of AP in the SDs. It is worth noting that most AP remained spherical in shape after the SD was prepared. In addition, PUE was better dispersed as AP was increased, as shown in Fig. 4d–h.

The DSC results are shown in Fig. 5. PUE exhibited two endothermic peaks at 121.4 and 213.0°C, which are characteristic of water and PUE, respectively. The DSC analysis of the PM (1:1) revealed that the endothermic peak characteristic of PUE was present at its expected position, indicating that PUE existed in a crystalline form. However, the endothermic peaks of PUE were significantly altered in all tested SD formulations. The endothermic peak at 213.0°C disappeared as the concentration of AP increased, which suggested that the crystallinity of PUE decreased in the SD vehicles because of its transformation to the amorphous state.

XRD studies were performed to investigate the crystal morphology of the drug. The XRD patterns shown in Fig. 6 indicate the presence of several distinct diffraction peaks for PUE, illustrating its crystalline nature. Various diffraction peaks were also observed for the PUE crystals in the spectra of the PM, which disappeared in the XRD patterns of the SDs. These data also suggest that PUE existed in an amorphous state in the SDs.

The amounts of residual organic reagents in the PUE-AP SDs (RDS 1:3) are listed in Table II, which showed lower than the common limits for residual solvents in the Chinese Pharmacopoeia [19].

In Vitro Release

The *in vitro* release of PUE and the SDs was compared, and the results are shown in Fig. 7. Approximately 35% of the drug was released from the PUE powders within 5 min, and the *in vitro* release percentage reached only 65% at the end of sampling (60 min). However, the release of the drug from the SDs was faster than those from the PUE powder groups. The percentage of drug release increased as the RDS decreased. Specifically, the SDs with an RDS of 1:2 and 1:3 showed 69 and 89% dissolution, respectively, in the first 5 min, whereas an almost complete release occurred from the SD formulations with an RDS of 1:5 and 1:10 at the final time point. However, the drug release percentage did not significantly increase for the SDs with an RDS ranging from 1:5 to 1:10.

Stability Test

The appearance of the stored samples was similar to that of the initial freshly prepared sample. As shown in Tables III and IV, the content of PUE after storage was measured, and

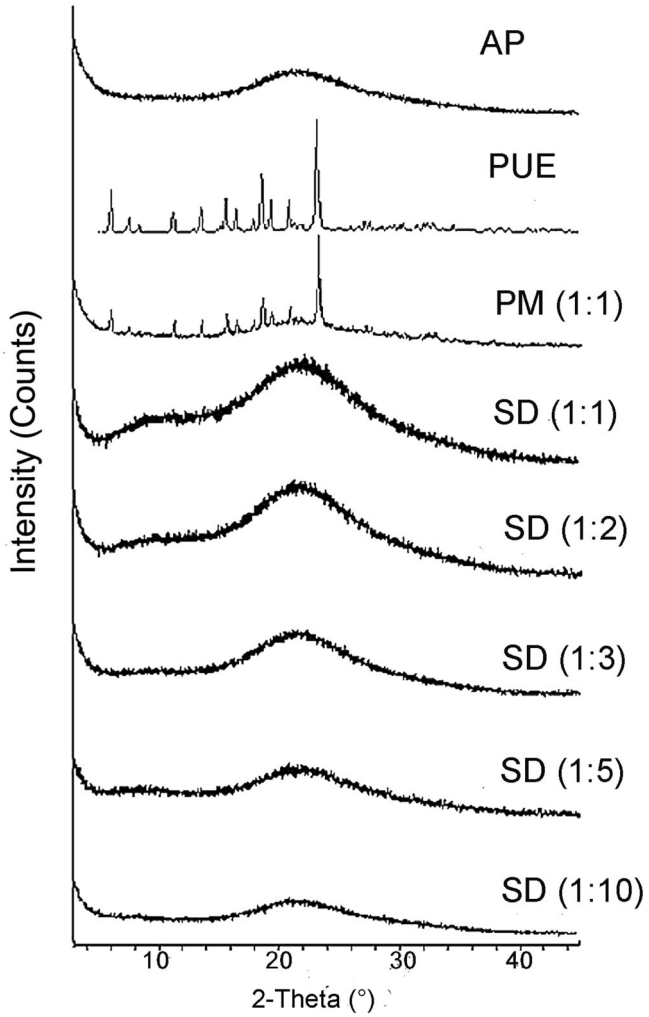

Fig. 6. X-ray diffractograms of PUE, AP, PUE-AP PM, and PUE-AP SDs

the values of the RSD were less than 3%, indicating that the stability of the drug stability was good.

The dissolution profiles of the PUE-AP SDs after storage are shown in Figs. 8 and 9. Drug dissolution from the SDs with RDS of 1:3, 1:5, and 1:10 was more than 85% within 15 min, indicating that there were no significant changes in the drug dissolution profile. The similarity factor (f_2) was calculated and used to identify the dissimilarities between the dissolution profiles of the stored and freshly prepared PUE-AP SD formulations. The dissolution profiles of the SDs with RDS of 1:2 from the 3-month accelerated aged samples and the 6-month long-term aged samples were comparable to those of the fresh tablets, as the f_2 values were

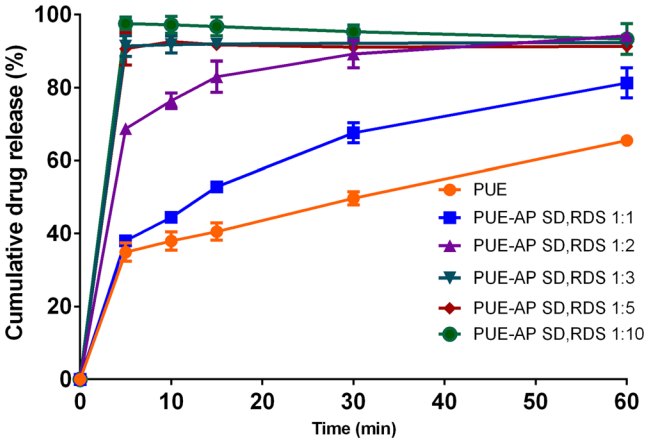

Fig. 7. *In vitro* release profiles of PUE-AP SDs with various RDS. Each point represents the mean ± standard deviation ($n = 3$)

greater than 50, indicating that the stability of the SDs was good.

Additionally, the results of the DSC (Fig. 10) and XRD (Fig. 11) studies demonstrated that PUE remained in an amorphous state in the PUE-AP SDs, thus proving that the presence of AP in the formulations can improve the physical stability of PUE.

Comparison of SDs Prepared by Different Carrier Materials

Preparation Process

As indicated in Table V, the strategy used to prepare the three SD formulations was simple, and it can be carried out using conventional equipment. The preparation process using AP was simpler and the rate of drug dissolution was higher than those of the commonly used carrier material, PVP.

The flowability of all the SD formulations the using compressibility index and the ratio of bulk density to tap density were determined. The results demonstrated that the CI % values of the PUE-AP SDs were the lowest among the three SD formulations (less than 20). Similarly, the angle of repose of the PUE-AP SDs was the smallest, while that of the PUE-EY-CD1 SDs was the largest. Compared with the SDs with the conventional hydrophilic silica carrier EY-CD1, the SDs with AP as the carrier material had a higher density and better fluidity. In addition, the hygroscopic rates of PUE-AP SDs and PUE-PVP SDs were the lowest and highest, respectively, among the tested formulations. Moreover, the agglomeration phenomenon occurred in PUE-PVP SDs, indicating that the AP-based SDs had a lower hygroscopicity than the EY-CD1- and PVP-based SDs.

Table II. The Residual Organic Solvents in PUE-Loaded SDs

Sample	Methanol (%)	Ethanol (%)	Dichloromethane (%)
PUE-AP SDs	0.01	0.05	ND (< 0.01%)
PUE-PVP SDs	0.01	3.50	ND (< 0.01%)
PUE-EY-CD1 SDs	ND (< 0.01%)	0.03	ND (< 0.01%)

PUE, puerarin; *AP*, AEROPERL® 300 Pharma; *SDs*, solid dispersions; *ND*, less than detection limit or report limit

Table III. The Content of Puerarin in SDs Before and After the Accelerated Test ($n = 3$)

PUE:AP	The content of PUE in SDs (%)				RSD (%)
	0 month	1 months	2 months	3 months	
1:10	6.93 ± 0.21	6.98 ± 0.13	6.87 ± 0.13	6.95 ± 0.21	1.41
1:5	11.23 ± 0.46	11.02 ± 0.24	11.24 ± 0.14	10.90 ± 0.20	2.25
1:2	20.17 ± 0.11	20.3 ± 0.21	20.37 ± 0.12	19.90 ± 0.15	1.05
1:1	35.68 ± 1.30	35.44 ± 0.23	35.05 ± 0.11	35.57 ± 0.28	1.70

PUE, puerarin; *AP*, AEROPERL® 300 Pharma; *SDs*, solid dispersions; *RSD*, relative standard deviation

Headspace gas chromatography–mass spectrometry was used to test the residual organic reagents for the three SD samples. As shown in Table II, the amounts of residual organic reagents in PUE-AP SDs and PUE-EY-CD1 SDs were lower than the common limits for residual solvents in the Chinese Pharmacopoeia [19], but the content of ethanol in PUE-PVP SDs exceeded the standard limitation, likely because it was difficult to completely evaporate the ethanol from the finished PUE-PVP SDs because of they were film-like material with a dense structure. However, both PUE-AP SDs and PUE-PVP SDs, which had loose structures, were easily volatilized because of their large pores.

The DSC results are shown in Fig. 12. The physical mixture of the two carrier materials and the PUE both exhibited a characteristic endothermic peak at its expected position, indicating that PUE existed in a crystalline form. When the solid dispersion was formed, the characteristic endothermic peak of PUE disappeared, indicating that PUE existed in the amorphous state in SD vehicles. The XRD results (Fig. 13) were consistent with those of the DSC analysis.

In Vitro Release of PUE from SDs Formed by Different Carrier

The *in vitro* drug release percentage from the PUE-AP and PUE-EY-CD1 SDs was significantly higher than that from the PUE-PVP K30 SDs. Unlike the SDs prepared with porous, water-wettable AP and EY-CD1 media, the PVP-based SDs tended to form a polymer membrane with a dense surface and small intermolecular porosity in the aqueous dissolution medium, which can potentially reduce the rate of drug release during the experimental period (Fig. 14).

Table IV. The Content of Puerarin in SDs Before and After 6 Months ($n = 3$)

PUE:AP	The content of PUE in SD (%)		RSD (%)
	0 month	6 months	
1:10	6.93 ± 0.21	7.02 ± 0.34	2.27
1:5	11.23 ± 0.46	11.33 ± 0.13	2.96
1:3	16.07 ± 0.44	16.43 ± 0.47	0.45
1:2	20.17 ± 0.11	20.44 ± 0.27	0.85
1:1	35.68 ± 1.30	35.96 ± 0.28	2.62

PUE, puerarin; *AP*, AEROPERL® 300 Pharma; *SD*, solid dispersion; *RSD*, relative standard deviation

In Vivo Pharmacokinetics

The results of the *in vivo* pharmacokinetics study were consistent with those of the *in vitro* drug release analysis. The plasma concentration–time curves for PUE in rats ($n = 6$) after the oral administration of PUE powder and PUE-loaded SDs (100 mg/kg of PUE) are shown in Fig. 15, and the pharmacokinetic parameters are listed in Table VI. Among all the tested formulations, the groups that were administered PUE-AP SDs exhibited the shortest time of maximum concentration (T_{max}), highest maximum plasma concentration (C_{max}), and the largest area under the concentration–time curve (AUC). The drug plasma concentration of the AP-based SD groups was significantly higher than those of the PUE and PUE-PVP groups. The $AUC_{(0-\infty)}$ of the AP-based groups was 2.05 and 2.01 times higher than that of API (PUE) and PVP K30-formed SDs, respectively. However, there was no significant difference between the $AUC_{(0-\infty)}$values of the PUE-AP SD groups and those of the PUE-EY-CD1 SD groups.

DISCUSSION

The results of the *in vitro* drug release test and the *in vivo* pharmacokinetic study demonstrated that as a carrier material, AP can effectively improve the dissolution rate and bioavailability of PUE. Moreover, the *in vitro* dissolution rate of PUE increased as the concentration of AP was increased for the three following reasons. First, according to the Noyes–Whitney equation, $dC/dt = DA(C_s - C_t)/h$ [20], where dC/dt is the dissolution rate, D is the diffusion coefficient, h is the thickness of the diffusion layer, A is the surface area available for dissolution, C_s is the solubility of the drug in the dissolution medium, and C_t is the drug concentration at a certain time, the saturation solubility and dissolution rate of a drug can be improved by increasing its surface area. The particles of AP are micron-sized and have a large specific surface area, and they can therefore increase the surface area of PUE by dispersing it, thus improving the dissolution rate. Second, the surface of AP particles contains silica hydroxyl [21], which is hydrophilic in nature. AP also contains interlinked pore channels, which can improve the wettability of insoluble drugs, reduce the contact angle, and increase the dissolution rate of the drug. Third, the enhanced solubility is a result of the disordered structure of the amorphous solid that offers a lower thermodynamic barrier

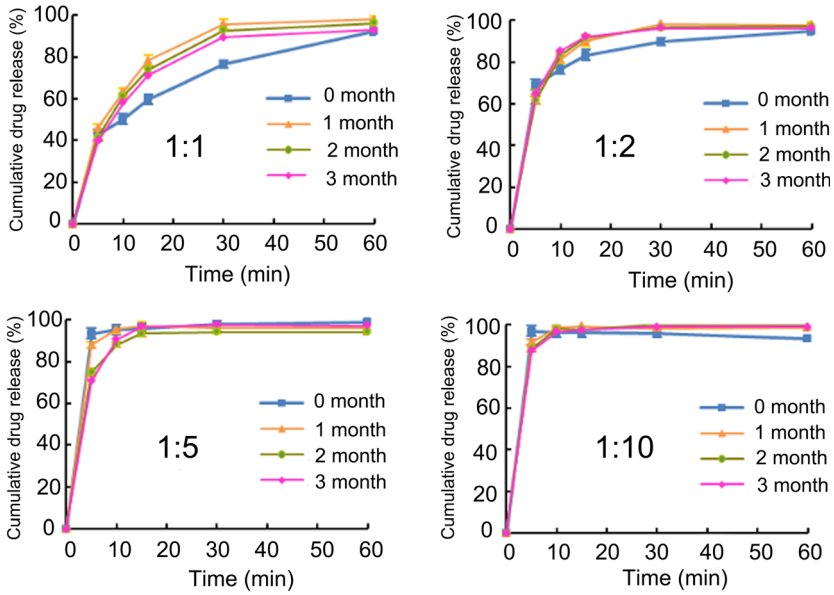

Fig. 8. *In vitro* release profiles of puerarin in SD before and after accelerated test. Each point represents the mean ± standard deviation ($n = 3$)

to dissolution and formation of a dispersion by adsorbing the drug into the pores of the porous silica carrier. An amorphous formulation system dissolves at a faster rate because of its higher internal energy and superior molecular motion. Amorphous drugs can have as much as 10–1600-fold higher solubility than their crystalline forms [22]. The results of the DSC and XRD studies showed that the amorphous PUE in the SD formulations exhibited better dissolvability than the crystalline poorly water-soluble drugs.

Aging is a common issue for SD formulations. Drugs are usually thermodynamically unstable in the amorphous

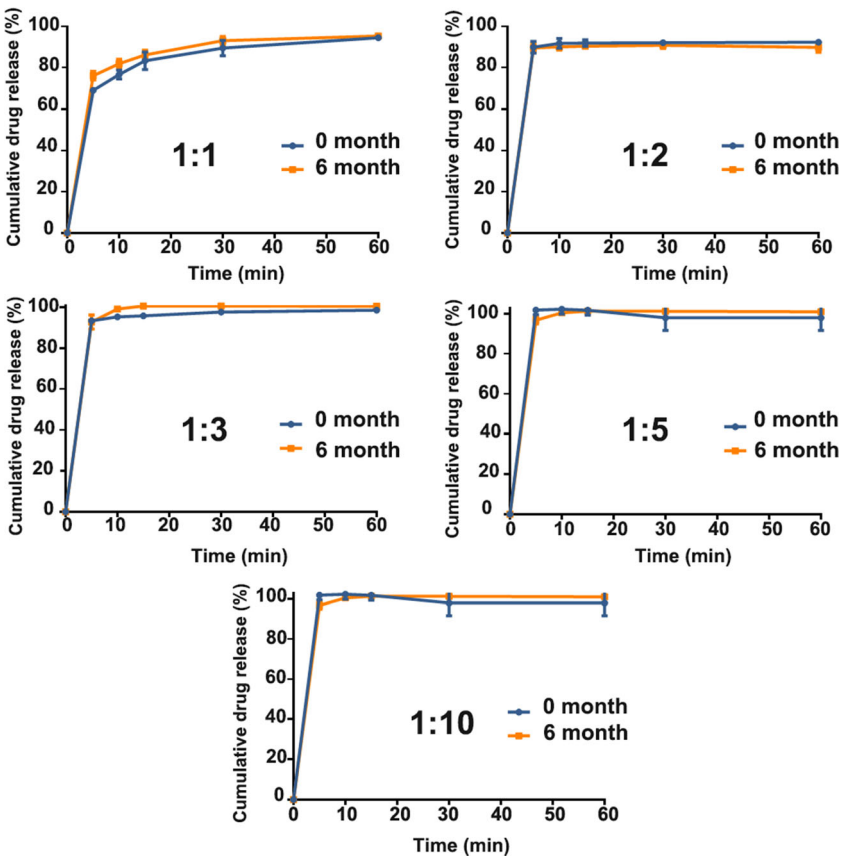

Fig. 9. *In vitro* release profiles of PUE in SD after being stored at room temperature for 0 and 6 months. Each point represents the mean ± standard deviation ($n = 3$)

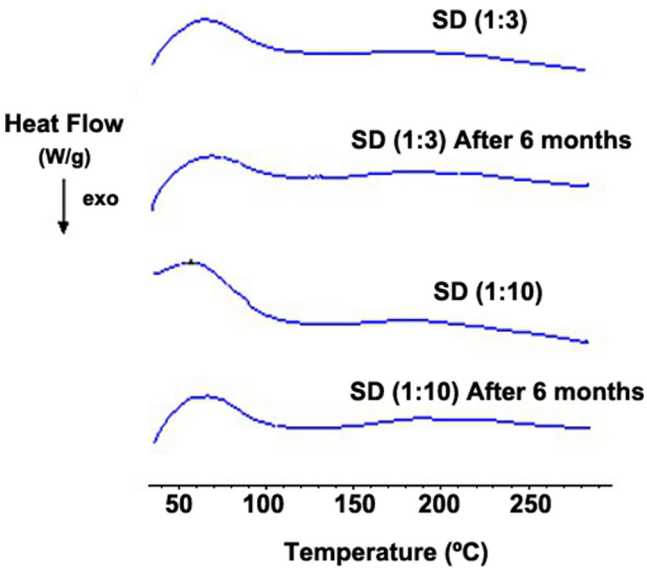

Fig. 10. DSC curves of PUE-AP SDs after being stored at room temperature for 0 and 6 months

state and tend to transform into the stable crystalline state. After a period of time, the drug molecules or crystallites are likely to migrate and aggregate, which can reduce drug dispersion and dissolution from the SDs. The PUE-AP SDs were prepared in this study using the solvent method, wherein the solvent was evaporated and PUE was adsorbed into the pore channels of AP, leaving insufficient space in the tiny pores for nucleation and crystal growth. The spatial constraint effect may prevent the recrystallization of drug molecules during its shelf life [23]. Additionally, the large internal surface area of mesoporous silica exists in an unstable state because of the high surface free energy. The silanol groups distributed on the internal surface of mesoporous silica can

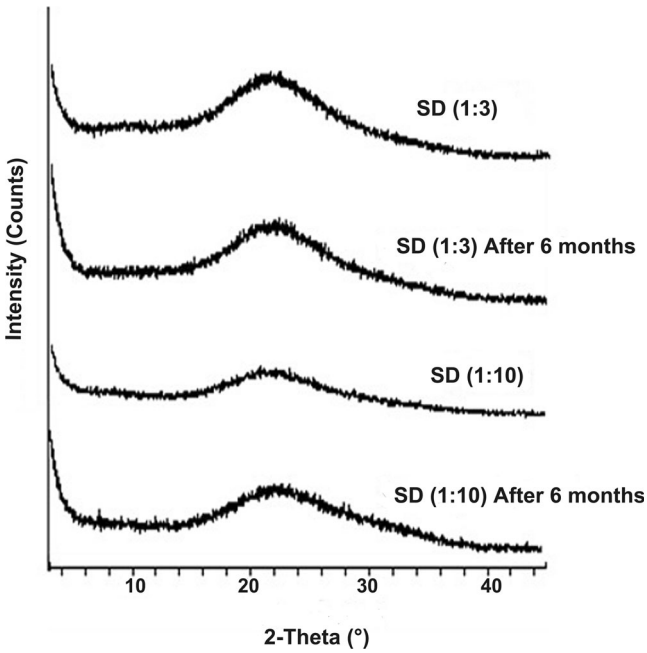

Fig. 11. X-ray diffractograms of PUE-AP SDs after being stored at room temperature for 0 and 6 months

Table V. Comparison of Different Carriers for Preparing SDs

	AP	PVP K30	EY-CD1
Preparation time (h)	3–4	6–7	3–4
Cumulative drug release (%) of 10 min	90	40	94
CI (%)	15.00 ± 0.01	19.31 ± 0.03	30.67 ± 0.02
Angle of repose (°)	31.91 ± 0.64	38.28 ± 0.93	48.30 ± 0.76
Hygroscopic rate (%)	0.16 ± 0.01	1.01 ± 0.14	0.28 ± 0.05

CI, Carr's compressibility index

interact with the drug molecules *via* H-bonds, thus allowing the system to progress to a lower free energy state as a whole [24]. Previous reports have demonstrated that the formation of hydrogen bonds between the drug molecules and mesoporous silica can effectively inhibit the recrystallization of the drug, improve the physical stability [25], and increase the dissolution rate of the drug [26]. In this study, PUE may have been adsorbed on the internal surface of AP in its amorphous state. Furthermore, the PUE molecules may have combined with the silanol groups of AP in the form of hydrogen bonds, resulting in a high free energy system prone to assuming a stable state. As expected, the characteristics of the stored samples were similar to those of the freshly prepared formulation.

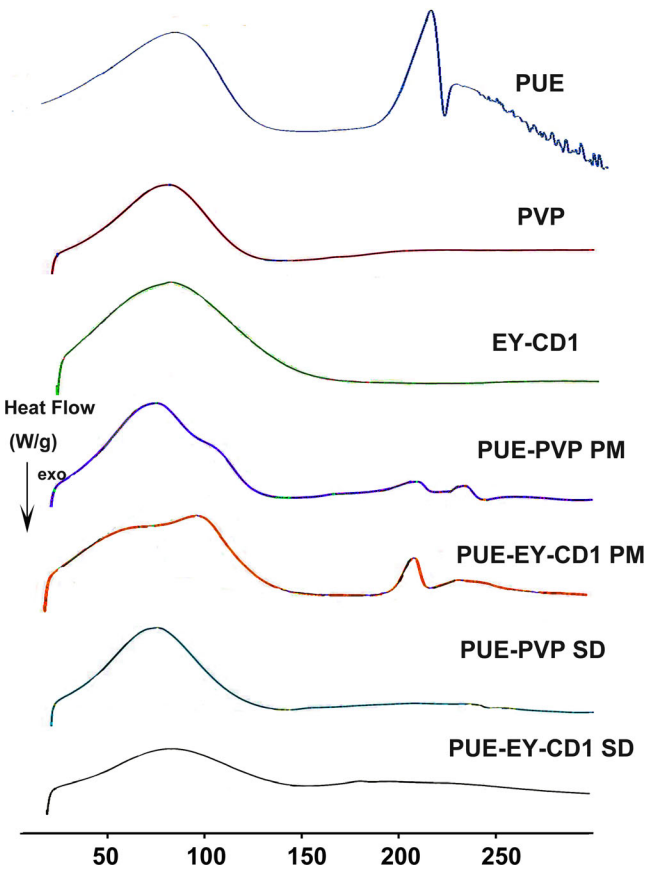

Fig. 12. DSC of PVP, EY-CD1, physical mixture with PUE (PM), and PUE-PVP SDs, PUE-EY-CD1 SDs

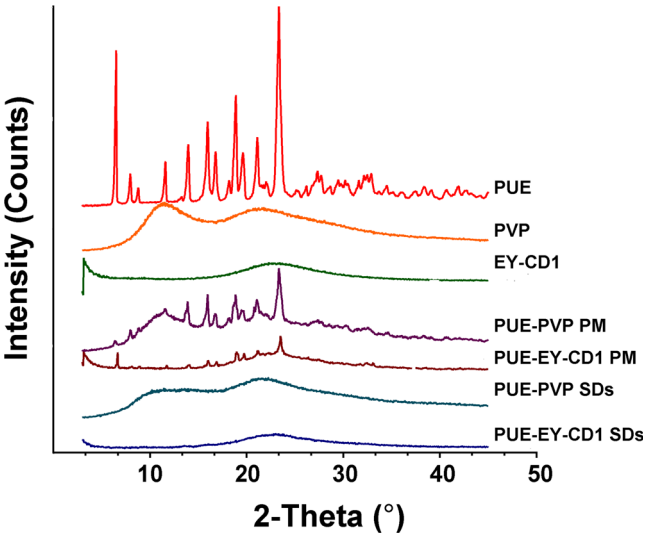

Fig. 13. X-ray diffractograms of PVP, EY-CD1, physical mixture with PUE (PM), and PUE-PVP SDs, PUE-EY-CD1 SDs

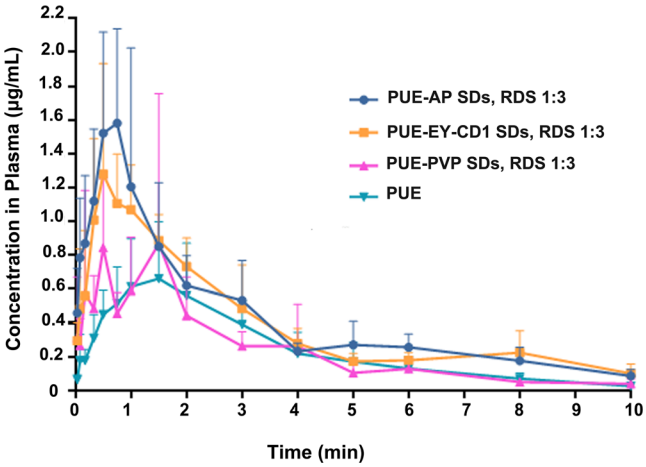

Fig. 15. Mean plasma concentration–time curves for puerarin (PUE) in rats after oral administration of the PUE powder (PUE) and PUE-loaded solid dispersions (SDs), equivalent to 100 mg/kg of PUE ($n = 6$). Values are the mean ± standard deviation ($n = 6$ per group per time point)

Different SD preparation strategies, including spray drying [27, 28], mechanical milling [29], freeze drying [30], hot melt extrusion [31], and supercritical fluid precipitation [32], have been developed to enhance the dissolution rate of poorly soluble drugs. However, most of these technologies have drawbacks, including scale-up issues and economic challenges. In this study, the PUE SDs were prepared with various adsorbents using the solvent method. The preparation strategy employed herein was a simple and high-drug–loading procedure and would be easy to industrialize.

In this study, SDs of three different carrier materials, PVP, silica EY-CD1, and AP, were compared with one another in terms of the *in vitro* dissolution rate and *in vivo* bioavailability during preparation. PVP K30 is the most frequently used carrier material for preparing SDs. Although PUE-PVP SDs formulated with an RDS of 1:3 increased the dissolution rate of PUE, there was no significant difference in the bioavailability of PUE in this case. The preparation of the PUE-PVP SDs involved refrigeration, decompression drying, pulverization, and grinding, which were time-consuming steps. Studies have demonstrated that SDs prepared with PVP are viscous in nature and sensitive to humidity during storage [33, 34]. Generally, the larger the amount of PVP, the higher is the absorption of moisture, which in turn can result in the precipitation and crystallization of the drug. In this study, we observed that the PUE-PVP SDs easily absorbed moisture and agglomerated, which could affect the physical stability of PUE.

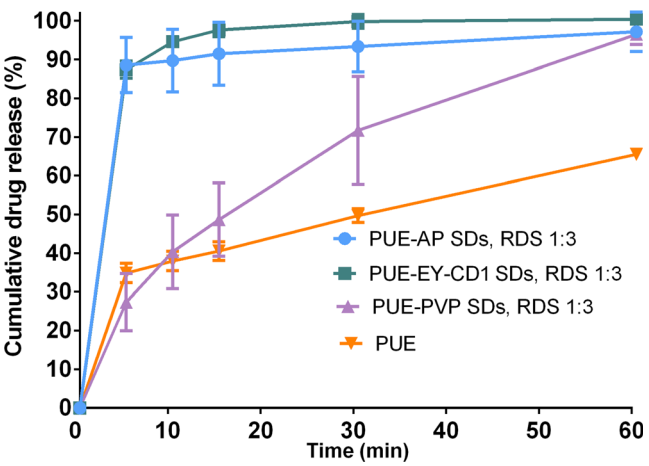

Fig. 14. *In vitro* release profiles of PUE-loaded SDs formed by different matrix. Each point represents the mean ± standard deviation ($n = 3$)

Although the SDs prepared with the EY-CD1 carrier exhibited improved dissolution rates and PUE bioavailability, the experimental results demonstrated that the SDs prepared with AP had the smallest angle of repose and Carr's compressibility index value, and these were significantly better than those of the EY-CD1 powder. The angle of repose reflects the dynamic fluidity of the powder, which is primarily related to particle morphology, particle size distribution, and water content of the powder. A powder is regarded as having poor flowability when the angle of repose is greater than 45°. The Carr's compressibility index reflects the stacking property and filling performance of the material, and a small Carr's compressibility index value is indicative of a strong filling property. According to the evaluation standards of the US Pharmacopoeia [35], flowability and filling ability are improved when Carr's compressibility index is less than 25% and can be used for production. As shown in Table IV, the angle of repose for PUE-EY-CD1 SD powders was greater than 45°, and Carr's compressibility index was more than 30%. EY-CD1 possesses an irregular block structure [36] and exhibits a poorer fluidity and lower filling ability after drug loading than the PUE-AP SD powders, making it disadvantageous for preparing oral SDs. AP has a smooth surface with a spherical shape and retains good fluidity and filling property after drug loading. The drug-loading process employed in this study was simple and fast.

Table VI. The Main Pharmacokinetic Parameters of PUE Powder and PUE-Loaded SDs in Rats ($n = 6$)

Parameters	PUE	PUE-AP SDs	PUE-EY-CD1 SDs	PUE-PVP SDs
T_{max} (h)	0.917 ± 0.624	0.708 ± 0.188	1.056 ± 0.993	0.778 ± 0.574
C_{max} (mg/L)	0.734 ± 0.338$^{▲}$	1.896 ± 0.538**	1.503 ± 0.548*	1.406 ± 0.512*
$t_{1/2}$ (h)	2.360 ± 1.163	4.884 ± 4.581	3.323 ± 1.884	2.204 ± 0.760
MRT_{0-t} (h)	2.951 ± 0.284	2.930 ± 0.379	3.046 ± 0.444	2.618 ± 0.382
$MRT_{0-\infty}$ (h)	3.42 ± 0.813	5.455 ± 1.457	4.079 ± 1.431	3.105 ± 0.521
AUC_{0-t} [(mg/L)·h]	2.432 ± 1.042	4.280 ± 0.910$^{**▲▲}$	3.968 ± 0.522$^{**▲▲}$	2.553 ± 0.691
$AUC_{0-\infty}$ [(mg/L)·h]	2.598 ± 1.123	5.323 ± 3.870$^{**▲▲}$	4.943 ± 1.308$^{**▲▲}$	2.646 ± 0.669
Relative bioavailability (%)	–	2.05	1.90	1.02

T_{max}, time of maximum concentration; C_{max}, maximum plasma concentration; $t_{1/2}$, half-life of elimination; $AUC_{0-\infty}$, area under the concentration–time curve; AUC_{0-t}, area under the concentration–time curve from time 0 to the last sampling time
$^{*}p < 0.05$, $^{**}p < 0.01$, *vs. PUE;* $^{▲}p < 0.05$, $^{▲▲}p < 0.01$, *vs. PUE-PVP SDs*

CONCLUSION

The use of AP-based SDs as the carrier of PUE effectively improved its drug dissolution. Additionally, an improved bioavailability of PUE was successfully achieved in this study. It can therefore be concluded that AP is a promising matrix for the preparation of SDs for drugs with poor water solubility.

FUNDING INFORMATION

This study was financially supported by Evonik Specialty Chemicals (Shanghai) Co., Ltd. and the National Natural Science Foundation of China (81603308).

COMPLIANCE WITH ETHICAL STANDARDS

All the animal experiments were carried out in accordance with the guidelines of the National Act on the Use of Experimental Animals and were approved by the local ethics committee (SCXK:2013-0016).

PUBLISHER'S NOTE

Springer Nature remains neutral with regard to jurisdictional claims in published maps and institutional affiliations.

REFERENCES

1. Rowe RC, Sheskey PJ, Cook WG, Fenton ME. Handbook of pharmaceutical excipients. 7th ed. London: The Pharmaceutical Press; 2012.
2. Meer T, Fule R, Khanna D, Amin P. Solubility modulation of bicalutamide using porous silica. J Pharm Invest. 2013;43:279–85.
3. Riikonen J, Xu WJ, Lehto VP. Mesoporous systems for poorly soluble drugs—recent trends. Int J Pharm. 2018;536:178–86.
4. Planinšk O, Kovačič B, Vrečer F. Carvedilol dissolution improvement by preparation of solid dispersions with porous silica. Int J Pharm. 2011;406:41–8.
5. Miura H, Kanebako M, Shirai H, Nakao H, Inagi T, Terada K. Enhancement of dissolution rate and oral absorption of a poorly water-soluble drug, K-832, by adsorption onto porous silica using supercritical carbon dioxide. Eur J Pharm Biopharm. 2010;76:215–21.
6. Li TT, Geng TJ, Md A, Banerjee P, Wang B. BoNovel scheme for rapid synthesis of hollow mesoporous silica nanoparticles (HMSNs) and their application as an efficient delivery carrier for oral bioavailability improvement of poorly water-soluble BCS type II drugs. Colloids Surf B: Biointerfaces. 2019;176(2):185–93.
7. Maleki A, Kettiger H, Schoubben A, Rosenholm JM, Ambrogi V, Hamidi M. Mesoporous silica materials: from physico-chemical properties to enhanced dissolution of poorly water-soluble drugs. J Control Release. 2017;262:329–47.
8. Shen SC, Ng WK, Chia LS, Dong YC, Tan RB. Applications of mesoporous materials as excipients for innovative drug delivery and formulation. Curr Pharm Des. 2013;19(35):6270–89.
9. Wei QH, Keck CM, Müller RH. Oral hesperidin—amorphization and improved dissolution, properties by controlled loading onto porous silica. Int J Pharm. 2017;518(1–2):253–63.
10. Pawar JN, Desai HR, Moravkar KK, Khanna DK, Amin PD. Exploring the potential of porous silicas as a carrier system for dissolution rate enhancement of artemether. Asian J Pharm Sci. 2016:760–70.
11. Alam MA, Ali R, Al-Jenoobi FI, Al-Mohizea AM. Solid dispersions: a strategy for poorly aqueous soluble drugs and technology updates. Expert Opin Drug Deliv. 2012;9(11):1419–40.
12. Bikiaris DN. Solid dispersions, part I: recent evolutions and future opportunities in manufacturing methods for dissolution rate enhancement of poorly water-soluble drugs. Expert Opin Drug Deliv. 2011;8:1501–19.
13. Gao Q, Yang B, Ye ZG, Wang J, Bruce IC, Xia Q. Opening the calcium-activated potassium channel participates in the cardioprotective effect of puerarin. Eur J Pharmacol. 2007;574:179–84.
14. Zhou YX, Zhang H, Peng C. Puerarin: a review of pharmacological effects. Phytother Res. 2014;28(7):961–75.
15. Wei SY, Chen Y. Xu XY. Progress on the pharmacological research of puerarin: a review. Chin J Nat Med. 2014;12(6):407–14.
16. Jiang XL, Jia YT, Zhang LK, Tian R, Teng YZ. Optimization of self-microemulsifying drug delivery system for puerarin by central composite design-response surface methodology. J Third Mil Med Univ. 2012;34(14):1414–7.
17. Khan AW, Kotta S, Ansari SH, Sharma RK, Ali J. Enhanced dissolution and bioavailability of grapefruit flavonoid naringenin by solid dispersion utilizing fourth generation carrier. Drug Dev Ind Pharm. 2015;41(5):772–29.
18. Seo SW, Han HK, Chun MK, Choi HK. Preparation and pharmacokinetic evaluation of curcumin solid dispersion using Solutol® HS15 as a carrier. Int J Pharm. 2012;424:18–25.
19. Chinese Pharmacopoeia Commission. Pharmacopoeia of the People's Republic of China (Volume IV). In: General rule; 2015. p. 0861.

20. Hattori Y, Haruna Y, Otsuka M. Dissolution process analysis using model-free Noyes-Whitney integral equation. Colloids Surf B: Biointerfaces. 2013;102(1):227–31.
21. Evonik, 2012. AEROSIL and AEROPERL colloidal silicon dioxide for pharmaceuticals technical information.
22. Hancock BC, Parks M. What is the true solubility advantage for amorphous pharmaceuticals? Pharm Res. 2000;17(4):397–404.
23. Qian KK, Bogner RH. Application of mesoporous silicon dioxide and silicate in oral amorphous drug delivery systems. J Pharm Sci. 2012;101(2):444–63.
24. Vogt FG, Roberts-Skilton K, Kennedy-Gabb SA. A solid-state NMR study of amorphous ezetimibe dispersions in mesoporous silica. Pharm Res. 2013;30(9):2315–31.
25. Li X, Peng H, Tian B, Gou J, Yao Q, Tao X, et al. Preparation and characterization of azithromycin – Aerosil 200 solid dispersions with enhanced physical stability. Int J Pharm. 2015;486(1–2):175–84.
26. Chauhan B, Shimpi S, Paradkar A. Preparation and evaluation of glibenclamide-polyglycolized glycerides solid dispersions with silicon dioxide by spray drying technique. Eur J Pharm Sci. 2005;26(2):219–30.
27. Singh A, Van den Mooter G. Spray drying formulation of amorphous solid dispersions. Adv Drug Deliv Rev. 2016;100:27–50.
28. Pawar JN, Shete RT, Gangurde AB, Moravkar KK, Javeer SD, Jaiswar DR, et al. Development of amorphous dispersions of artemether with hydrophilic polymers via spray drying: physicochemical and in silico studies. Asian J Pharm Sci. 2016;11(3):385–95.
29. Zhong L, Zhu X, Yu B, Sn W. Influence of alkalizers on dissolution properties of telmisartan in solid dispersions prepared by cogrinding. Drug Dev Ind Pharm. 2014;40(12):1660–9.
30. He Y, Ho C. Dispersions: solid amorphous utilization and challenges in drug discovery and development. J Pharm Sci. 2015;104(10):3237–58.
31. Alshahrani SM, Lu W, Park JB, Morott JT, Alsulays BB, Majumdar S, et al. Stability-enhanced hot-melt extruded amorphous solid dispersions via combinations of Soluplus® and HPMCAS-HF. AAPS PharmSciTech. 2015:1–11.
32. Ma XY, Williams RO. Characterization of solid amorphous dispersions: an update. J Drug Deliv Sci Technol. 2019;50:113–24.
33. Rumondor AC, Stanford LA, Taylor LS. Effects of polymer type and storage relative humidity on the kinetics of felodipine crystallization from amorphous solid dispersions. Pharm Res. 2009;26(12):2599–606.
34. Li W, Buckton G. Using DVS-NIR to assess the water sorption behaviour and stability of a griseofulvin/PVP K30 solid dispersion. Int J Pharm. 2015;495(2):999–1004.
35. US Pharmacopoeia (USP 41), 2018.
36. Ye BN, Wang Z, Feng NP. Solidification of patchouli oil with fumed silica AEROPERL® 300 Pharma. Chin J New Drugs. 2015;24(1):80–4.